Available online at www.sciencedirect.com
SCIENCE DIRECT®
Polymer 44 (2003) 7131–7141
polymer
www.elsevier.com/locate/polymer

Dilute solution behaviour of sodium polyacrylate chains in aqueous NaCl solutions

Ralf Schweins[1], Jutta Hollmann[2], Klaus Huber*

Department Chemie und Chemietechnik, Fakultät für Naturwissenschaften, Universität Paderborn, Physikalische Chemie, Warburger Street 100, D-33098 Paderborn, Germany

Received 17 February 2003; received in revised form 4 July 2003; accepted 31 July 2003

Abstract

Combined static and dynamic light scattering was used to characterise a variety of sodium poly(acrylate) samples in dilute aqueous solutions with added NaCl. An increase of the NaCl content resulted in a decrease of the solvent quality. On the basis of these findings, two solvent conditions were selected for a detailed investigation of the coil size as a function of the molar mass M_w : aqueous 0.1 M NaCl represents a thermodynamically good solvent and aqueous 1.5 M NaCl is close to a Θ-solvent. If the NaCl content was kept within this range of 0.1 M ≤ [NaCl] ≤ 1.5 M, a single Kuhn segment length of $l_k = 4.2$ nm and an excluded volume parameter of $\omega_0 = -0.04$ for the corresponding neutral monomer [Muthukumar et al. Macromolecules 30; 1997: 8375] were able to adequately describe coil expansion as a function of the molar mass and the content of added salt. Towards lower salt contents, Muthukumar's approach which is based on the excluded volume parameter ω_0, the Kuhn segment length l_k and an effective charge density f became increasingly inadequate.

Keywords: Polyacrylic acid; Coil size; Light scattering

1. Introduction

Polyacrylic acid and its salts belong to the most frequently applied polyelectrolytes both in household and industry. They are applied as dispergators for inorganic pigments, scale inhibitors in laundry processes and thickening agents in water born formulations to name but a few examples. Thus, the technical relevance of polyacrylic acids created an early need for information on the dilute solution behaviour of sodium polyacrylate (NaPA) which includes the dependence of hydrodynamic radii R_h and radii of gyration R_g on chain length.

Though a number of pioneering studies on dilute solution behaviour of PA salts do exist [1–6], investigation of molar mass dependent coil size was usually based on viscosity measurements [3–6]. Results demonstrated [3–6] that the dependence of the hydrodynamic volume on the PA molecular weight was comparable to that of neutral polymers if the concentration of added salt was above 0.1 M. The respective power laws could be described satisfactorily by means of the two parameter theory established for neutral polymers. In line with this, water with 1.5 M NaBr at 15 °C could be identified as a Θ-state for fully neutralized NaPA, leading to the unperturbed dimensions of anionic PA coils [3,4]. For a degree of ionization lower than one third, the Θ-state was found to be $T = 32$ °C and 1.245 M NaCl [1].

Light sacttering (LS) experiments on aqueous NaPA were restricted to the investigation of various aspects of a few high molecular weight samples [1,7–10], but did not consider power laws of the radius of gyration or the hydrodynamic radius. Hara and Nakajima [7] represented a classical analysis of scattering intensities as a function of scattering angle and NaPA concentration. A single sample was investigated at three different added salt concentrations: 1.5 M KBr at $T = 15$ °C, 0.1 and 0.01 M NaCl. They recovered unperturbed dimension for NaPA at 1.5 M KBr. A decrease of the added salt content led to an increase of the second virial coefficient, which could be formally captured as an increase of solvent quality, in analogy to dilute

* Corresponding author.
E-mail address: huber@chemie.uni-paderborn.de (K. Huber)
[1] Present address: Institut Laue—Langevin, LSS Group, B.P. 156, 6, rue Jules Horowitz, F-38042 Grenoble, cedex 9, France.
[2] Present address: Institut für Physikal. Chem., Universität Stuttgart, Pfaffenwaldring 55, D-70569 Stuttgart, France.

0032-3861/$ - see front matter © 2003 Published by Elsevier Ltd.
doi:10.1016/j.polymer.2003.07.005

solution behaviour of neutral polymers, thereby confirming the picture established by the early viscosity measurements on NaPA [3–6]. At the same time, Nagasawa et al. [8–10] extracted single chain behaviour of a partially neutralized polyacrylic acid sample at a varying level of added salt of 0.01 M KBr $\leq C_s \leq$ 0.5 M KBr. Experimental curves at the Θ-state could successfully be described by means of the Debye function for an unperturbed Gaussian chain [11]. Chain expansion due to a decrease in the concentration of added salt could be satisfactorily accounted for by a theoretical approach from Peterlin et al. based on Gaussian chains with excluded volume [12]. In addition, Nagasawa et al. [8–10] applied the worm like chain model [13], however, with much less success. This model allowed to account for chain expansion by simply increasing the persistence length instead of introducing excluded volume effects. Using a model of worm like chains with excluded volume was expected to be more appropriate but would be much more complicated. Nevertheless, it was applied somewhat later for other systems like PSS. A summary of the corresponding theoretical approaches including first applications can be found in an early review by Förster and Schmidt [14].

Aqueous salt solutions of PSS were also among the first systems for which power laws of the chain dimensions, expressed as R_g and R_h versus the weight averaged molar mass M_w,

$$R_g \sim M_w^{\nu}, R_h \sim M_w^{\nu} \tag{1}$$

were established. Whereas, Raziel and Eisenberg [15] published an R_g versus M_w relationship in 0.5 M NaCl as early as 1971, Wang and Yu [16] and later Tanahatoe and Kuil [17] presented corresponding power laws for R_h, covering a range of added salt of 0.002 M $\leq C_s \leq$ 3.16 M. In this regime, the highest salt concentration corresponded to a Θ-state for PSS. With the exception of the lowest salt concentration of 0.002 M phosphate buffer, the corresponding exponents lay close to $0.5 \leq \nu \leq 0.6$. As expected, the exponent approached 0.5 at the salt concentration representing the Θ-state. In the meantime similar relationships were published for other polyelectrolyte systems [18–21]. It is perhaps worth being mentioned that an exponent of 0.5 was reached for two systems which still exhibited positive second virial coefficients [19,21]. The exceptional power of combined static and dynamic LS techniques in this context was proven by Beer and Schmidt [22,23] on poly(vinylpyridine) (PVP) and quarternized derivatives thereof and by Norisuye et al. [24] on PSS. The former investigated coil dimensions as a function of its molar mass and of the concentration of added salts. They [22,23] developed exponents for R_g and R_h at a variety of different salt levels according to Eq. (1). Although a decrease of the exponent was observed with increasing salt content, exponents were slightly larger than 0.6 except for the highest salt concentrations. At the same time, combined LS gave access to the shape sensitive ratio

$$\rho = R_g/R_h \tag{2}$$

which revealed additional information on the conformation of the PVP chains. Norisuye et al. [24] presented molecular weight dependencies for the coil size of PSS at three different inert salt concentrations. At the lowest level of $C_s = 0.005$ M investigated by the authors, the exponents were larger than expected for the good solvent limit of flexible polymer chains. An overview of the respective exponents [15–24] is presented in Table 1.

To our surprise, only one light scattering work considered power laws for NaPA in aqueous salt solutions so far: Wiegand et al. [25] investigated several NaPA samples with different molar masses in 1.0 M NaCl by means of dynamic and static LS and compared the results with molecular dynamics simulation. Corresponding data are also included in Table 1. This persisting lack of data for a polyelectrolyte as technically relevant as NaPA motivated us to investigate the following questions: does a regime of added salt exist, in between which the solvent conditions can be varied from the good solvent limit to the Θ-state? Provided that such a regime exist, can the M_w dependence of the coil size be described by a set of two parameters? In which way does the amount of added salt then effect the two parameters? In order to answer these questions, the coil size of a single NaPA sample shall be measured in a concentration regime of 0.01 M $\leq C_s \leq$ 1.5 M and molar mass dependent coil dimensions of NaPA shall be investigated at two solvent conditions, in 0.1 and 1.5 M NaCl. The latter salt level was expected to be high enough to provide unperturbed dimensions for NaPA. All experiments were performed with a set of 6–9 NaPA samples being marginally polydisperse. All weight averaged molecular weights were roughly 20% larger than the corresponding number averaged values.

2. Experiments and data evaluation

2.1. Materials

Different samples of sodium poly(acrylate) were purchased from Polymer Standards Service, Mainz (Germany) and from Polysciences, Eppelheim (Germany). The samples covered a molecular weight range from 75,000 to 3,300,000 g/mol. All samples had a certified polydispersity of 1.5–1.6. Other chemicals (NaCl and NaOH) were purchased from Fluka, Buchs (Switzerland) with puriss. p. a. grade. Bidistilled water was generated by using a Heraeus apparatus which yields water with a conductivity below 0.1 μS/cm.

2.2. Determination of refractive index increments

Knowledge of refractive index increments is essential if

Table 1
Literature values for the exponent ν according to Eq. (1) for various polyelectrolyte systems in aqueous solution

Polyelectrolyte	C_s (mol/l)	ν for R_g	ν for R_h	R_g/R_h	Reference
PSS	0.5	0.64 ± 0.05			15
PSS	0.002 phosph. buffer		0.66		16
PSS	0.15		0.6		16
PSS	3.1 Θ-state		0.5		16
PSS	0.1		0.61 ± 0.04		17
PSS	0.05	0.63	0.63		24
PMTAC[a]	1.0	0.56			18
PDADMAC[b]	0.5		0.5		19
PIS[c]	0.5		0.59	1.62	20
NaPAMS[d]	0.05	0.5			21
NaPAMS	0.5	0.5			21
NaPA	0.5		0.55	1.47	25
Q-PVP[e]	0.1	0.59 ± 0.04	0.61 ± 0.02		22
Q-PVP	0.03	0.62 ± 0.02	0.65 ± 0.02		22
Q-PVP	0.01	0.68 ± 0.03	0.68 ± 0.03		22
Q-PVP	0.03	0.72 ± 0.03	0.71 ± 0.02		22
Q-PVP	0.001	0.73 ± 0.02	0.78 ± 0.02		22

[a] Poly(trimethylammoniummethylmethacrylate chloride).
[b] Poly(diallyldimethylammonium chloride).
[c] Sodium poly(isoprenesulfonate).
[d] Poly(2-acrylamido-2-methylpropanesulfonate).
[e] Poly(2-vinylpyridine) quaternized with benzyl bromide.

absolute values of the molecular weight and the second osmotic virial coefficient of polymers have to be calculated from LS experiments. For the determination of refractive index increments, a scanning differential refractometer, ScanRef monocolor from NFT GmbH, Göttingen (Germany) was used having a laser light source with a wavelength of 543.5 nm. The ScanRef refractometer operates according to the principle of a Michelson interferometer.

Each characterisation of a refractive index increment (dn/dc) was based on a series of seven different concentrations. Measurement of a series of samples took approximately 20 min. Usually, slight changes of temperature were observed within this time, which did not exceed 0.2 K. In order to correct for those changes, solvent was injected into the sample cell prior and after each measurement series. Temperature differences thus became visible by a difference between the initial and final solvent measurement which could be used to infer a drift of the signal. This drift was used to adequately correct the signals of all concentrations. Unfortunately, the interferometric detection principle does not allow to distinguish between a phase difference of x and of $(x + \lambda)$. In order to still receive absolute phase differences, at least one polymer concentration with a phase difference smaller than the laser wavelength had to be measured. This could be achieved with a polymer concentration lower than 0.5 g/l. Under the assumption that zero polymer concentration is equivalent to zero refractive index increment, a linear relationship was guessed. By means of this guess, the so-called modulo-π-correction then shifted all other refractive index differences correspondingly, resulting in a slope which corresponded to the refractive index increment ($\partial n/\partial c$).

Dilute solutions of polymers can be regarded as two phase systems: polymer free solvent and confined domains with monomer clouds from polymer chains. In case of polyelectrolytes dissolved in salt solutions, electrostatic interactions lead to an unequal distribution of the added salt among the two 'phases'. This effect, also denoted as Donnan effect, modifies the optical contrast of the dissolved polyelectrolyte chains against the saline solvent. The contrast now relevant for data evaluation in LS is the contrast between the polyelectrolyte domains and the polyelectrolyte free salt solution where the polyelectrolyte domains are in equilibrium with the surrounding salt solution. In order to distinguish this contrast from an ordinary refractive index increment, an index μ is used in $(dn/dc)_\mu$. The index indicates that the chemical potential of the added salt is the same in the pure solvent and the polyelectrolyte containing solution.

In the present paper both, dn/dc and $(dn/dc)_\mu$, was determined experimentally. In the former case solvent and NaPA solutions had the same NaCl concentration. In the latter case they had the same chemical potential for NaCl. Adjustment of chemical potentials was achieved by dialysing stock solutions of NaPA with salt solutions having the desired concentration of NaCl. In both cases a polymer stock solution was prepared and homogenised by gently rotating at room temperature for 6 days. Any dialysed stock solution was diluted with the salt solution which was equilibrated with the respective stock solution. When dealing with undialysed solutions, the stock solution was

directly used to generate a dilution series including 7 solutions. All dilution series were prepared the day before the refractive index increment measurement and stored on the cell housings of the differential refractometer before use.

For dialysis, cells similar to those described in Ref. [26] were built. The dialysis cells had two chambers, each having a volume of 25.5 cm^3. Dialysis was always carried out for 72 h under constant volume. As a membrane we used 'Thomapor Dialyseschlauch Standard' with a separation limit of 10,000 g/mol as well as 'Thomapor Dialyseschlauch Spezial' with a separation limit of 1000 g/mol, from Reichelt Chemietechnik, Heidelberg (Germany). Both membranes gave the same refractive index increment values.

The results of the refractive index increment measurements are summarised in Table 2. Clearly, the molar mass has no influence on the refractive index increment if $M_w \geq 170000$ g/mol. Thus, averaging of refractive index increments at constant chemical potential of NaCl led to $(dn/dc)_\mu = 0.1670$ and 0.1346 ml/g in 0.1 and 1.5 M NaCl, respectively. Those values are plotted in Fig. 1 together with values from literature [27]. All values can be fitted with the following empirical relation

$$\left(\frac{\partial n}{\partial c}\right)_\mu = 0.17139 - 0.04581 \cdot c + 0.01423 \cdot c^2 \quad (3)$$

By means of Eq. (3) $(dn/dc)_\mu$ values were interpolated within 0.01 M ≤ [NaCl] ≤ 1.5 M, which was successfully applied to determine the correct molecular weight and second osmotic virial coefficient data of the salt-dependent measurement series presented in Fig. 3.

2.3. Preparation of solutions for LS measurements

As explained in detail by Brüssau et al. [26], it is not necessary to dialyze the solutions used for light scattering experiments if $(dn/dc)_\mu$ is used for the evaluation of the scattering contrast. Stock solutions were prepared by dissolving the appropriate amount of an NaPA sample in a freshly prepared solvent. The solvent always has a pH of 9

Table 2
Refractive index increments of NaPA in aqueous solutions of NaCl

M_w (g/mol)	λ (nm)	[NaCl] (M)	dn/dc (ml/g)	$(dn/dc)_\mu$ (ml/g)
171000	543.5	0.1	0.172 ± 0.002	0.168 ± 0.006
491000	543.5	0.1	0.174 ± 0.006	0.167 ± 0.002
3150000	543.5	0.1	0.175 ± 0.003	0.167 ± 0.011
3150000	543.5[a]	0.1	0.184	0.166
3150000	633[a]	0.1		0.166
171000	543.5	1.5		0.147 ± 0.03
390000	543.5[a]	1.5		0.131
390000	633[a]	1.5		0.130
491000	543.5	1.5	0.178 ± 0.02	0.143 ± 0.02
907000	543.5	1.5	0.157 ± 0.005	0.120 ± 0.006
3150000	543.5	1.5	0.162 ± 0.008	0.136 ± 0.024
3150000	543.5[a]	1.5		0.140

[a] Experiments were performed in the laboratory of Prof. M Schmidt, Universität Mainz with the same type of instrument.

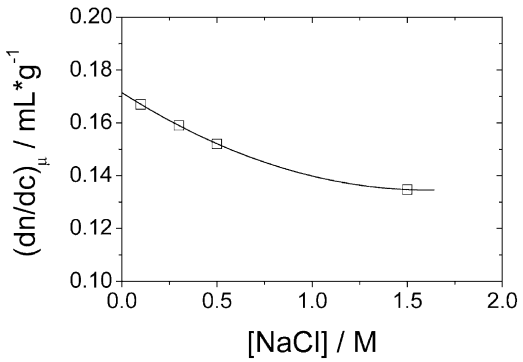

Fig. 1. Refractive index increments as a function of the concentration of added NaCl. The NaPA solutions were dialysed with the corresponding NaCl solutions prior to measurement. The line is a nonlinear fit according to Eq. (3).

and contains a distinct amount of NaCl. The stock solution was gently rotated at room temperature for 6 days. Finally, four additional concentrations were prepared from the stock solution by dilution with solvent. All five concentrations were directly filtered into the scattering cells through Millipore filters with a PVDF membrane. Depending on the coil size of the respective NaPA sample, pore sizes of 0.22 or 0.45 μm were used respectively. Polymer concentrations were given in g/l of NaPA.

2.4. Light scattering apparatus

All experiments were performed with an ALV 5000E Compact Goniometer System, Langen (Germany) with a multiple tau digital correlator, which allows to simultaneously measure static and dynamic light scattering in an angular range between 30° and 150°. A Nd:YAG laser with a power of 100 mW and a wavelength of 532 nm serve as a light source. The scattering intensity was guided to two photomultipliers with a monomode fiber. For all experiments, cylindrical scattering cells from Hellma, Müllheim (Germany) with an outer diameter of 20 M were used. All measurements were performed at 25 °C.

2.5. Data evaluation of static light scattering

In order to extract the weight averaged molecular weight M_w, the radius of gyration R_g and the second osmotic virial coefficient A_2 from SLS data, a double extrapolation to the NaPA concentration $c = 0$ and to scattering vector $q = 0$ is required. The basis of this evaluation is the Zimm [28] equation

$$\frac{K \cdot c}{\Delta R_\theta} = \frac{1}{M_w} + \frac{1}{3M_w} R_g^2 \cdot q^2 + 2A_2 c \quad (4)$$

with K being

$$K = \frac{4\pi^2}{\lambda_0^4 \cdot N_L} \left(n \frac{\partial n}{\partial c}\right)_\mu^2 \quad (5)$$

where λ_0, N_L, n and are the laser wavelength in vacuum,

Avogadro's number and the refractive index of the solvent respectively. ΔR_θ expresses the net scattering intensity of the dissolved polymer sample which is measured as a function of the NaPA concentration c and the scattering angle θ via the scattering vector q

$$q = \frac{4\pi n}{\lambda_0}\sin\frac{\theta}{2} \tag{6}$$

$n = 1.3363$ and $n = 1.3497$ was used as the refractive index of the solvent 0.1 M NaCl and 1.5 M NaCl respectively. Absolute Rayleigh ratios were referred to the Rayleigh ratio of $R = 2.737 \times 10^{-5}$ cm^{-1} for toluene at 298.15 K.

In our case $Kc/\Delta R_\theta$ exhibited a linear dependence on q^2 for all concentrations. Unlike to the linear q^2-dependences the dependences on c were non-linear if [NaCl] $\leq$ 1.5 M. An example is given in Fig. 2. Therefore a mixed data evaluation was performed: in a first step, we linearly extrapolated $Kc/\Delta R_\theta$ to $q^2 = 0$ at each concentration, yielding apparent molecular weights as the inverse intercepts and the apparent radii of gyration $R_{g,app}$ from the slopes. In a second step, we plotted the square root of each intercept as a function of the concentration according to Berry's method [29]

$$\sqrt{Kc/\Delta R_{\theta=0}} = 1/\sqrt{M_w} + A_2\cdot\sqrt{M_w}\cdot c \tag{7}$$

Weight averaged molar mass values M_w and second virial coefficients A_2 were extracted from the intercepts and slopes respectively. The radii of gyration of the polymer samples were evaluated according to two methods: (i) from the intercepts of a plot of $1/R_{g,app}$ as a function of NaPA concentration c; (ii) by extrapolating the slope of the q^2 dependences to $c = 0$ and multiplying the limiting slope with M_w. The second method turned out to be more practicable for the evaluation of the salt dependent scattering data where a large variation of the excluded volume effects occurred.

2.6. Data evaluation of dynamic light scattering

Dynamic Light Scattering (DLS) data were recorded as intensity-time correlation functions which were transformed into electric field-time correlation functions $g_1(q,t)$. They depend on the diffusion coefficient D of the dissolved polymers according to

$$g_1(t) = \int_0^\infty G(D)\cdot e^{-D\cdot t/q^2}\,dD \tag{8}$$

$G(D)$ is the resulting distribution function of D which can be evaluated by means of the CONTIN method developed by Provencher [30,31]. In the present publication CONTIN was only used to assure that the polymer samples exhibit single modes based on molecularly dissolved particles. All presented diffusion coefficients were gained from a cumulant fit [32] of $g_1(q,t)$. This fit describes the logarithm of $g_1(t)$ at constant q as a power series in t

$$\ln(g_1(q,t)) = \Gamma_0 - \Gamma_1\cdot t + \frac{\Gamma_2}{2!}\cdot t^2 - \frac{\Gamma_3}{3!}\cdot t^3 \tag{9}$$

where Γ_0, Γ_1, Γ_2 and Γ_3 are the cumulants. The first cumulant Γ_1 and the second cumulent Γ_2 are determined by the z-averaged diffusion coefficient D and the polydispersity index M_w/M_n, respectively.

$$D = \Gamma_1 q^2 \tag{10a}$$

$$\Gamma_2/\Gamma_1^2 = M_w/M_n \tag{10b}$$

In Eq. (10b), M_n is the number averaged molar mass of the polymer. All correlation functions resulted in polydispersity indices M_w/M_n independent of q and c. Averaged values lay close to $M_w/M_n = 1.2$ for all samples used in the present work. This value was much lower than the one being specified by the supplier. Diffusion coefficients were determined via extrapolation of D to $c = 0$ and $q^2 = 0$ according to [33]

$$D = D_0(1 + k_D\cdot c + C\cdot R_g^2\cdot q^2) \tag{11}$$

In Eq. (11), D_0 is the extrapolated diffusion coefficient, C is a dimensionless constant which depends on polydispersity and particle shape [33] and k_D is a constant describing the concentration dependence of D. Under Θ-conditions, k_D adopts negative values [34–36] and in good solvents k_D is positive [37,38].

Finally, D_0 is transformed into a hydrodynamically effective radius R_h by use of the Stokes–Einstein equation [38]

$$R_h = \frac{k\cdot T}{6\pi\cdot\eta}\cdot\frac{1}{D_0} \tag{12}$$

where k, T, η denote the Boltzmann constant, the temperature and the solvent viscosity respectively. $\eta = 897.86$ and $\eta = 1027.16$ μPa was used as solvent viscosity for 0.1 M NaCl and 1.5 M NaCl, respectively.

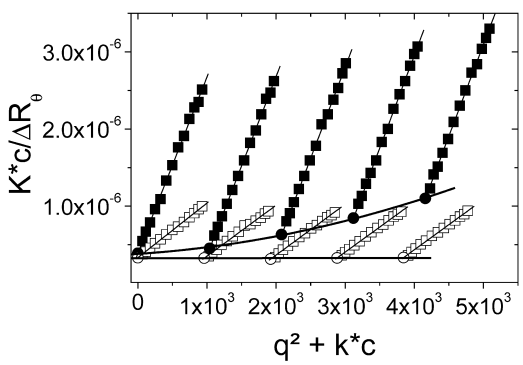

Fig. 2. Static light scattering diagrams of PA2 in aqueous salt solutions: (□) 1.5 M NaCl, (■) 0.1 M NaCl.

3. Results and discussion

3.1. Scaling laws

As early as 1951, Flory and Osterheld [1] could show that partially ionized polyacrylic acid in aqueous solution of an inert salt shrinks in size if the concentration of the inert salt is increased. This shrinking process can be pushed towards the unperturbed dimensions of the NaPA chains. Denoted as Θ-state for neutral polymers, a comparable state is reached for fully ionized NaPA at $T = 15$ °C and 1.5 M KBr [3,4].

In a first step, we established solvent conditions appropriate to represent the two limiting conditions 'good solvent' and 'Θ-solvent'. This was achieved by investigating a single sample at $M_w = 3.3 \times 10^6$ *g/mol* as a function of the NaCl content. The latter acts as an inert salt and screens the electrostatic interactions. Results are summarized in Fig. 3a–c. The second virial coefficient decreases from a value of $A^2 = 7.3 \times 10^{-4}$ *mol ml/g*^{2} at 0.1 M NaCl to a value of $A_2 \sim 0$ at 1.5 M NaCl. At the same time, the coil dimensions decreased by some 50%. Measurement of both radii allowed formation of the shape sensitive ratio according to Eq. (2) which, in the present case, decreased from 1.8 in 0.1 M NaCl to 1.5 in 1.5 M NaCl. For neutral polymers in good solvent, Akcasu and Benmouna [39] predicted a value of 1.86. A slightly lower value of 1.64 could be inferred from Barrett's calculation [40] of the geometric and hydrodynamic expansion coefficients [41]. For neutral chains under Θ-conditions, a significantly lower value of $\rho = 1.5$ was evaluated [42]. Experiments on neutral polymers with narrow molecular weight distributions confirmed this solvent quality dependent drop in ρ, but the experimental values were generally 15–25% lower than theoretically expected [41,43,44].

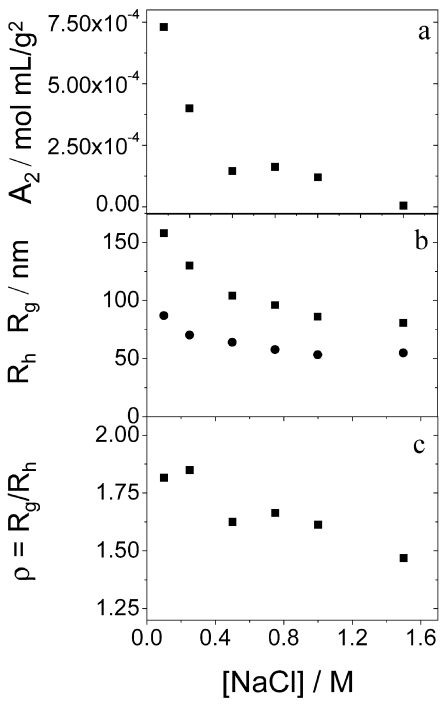

Fig. 3. Dilute solution properties of sample PA2 ($M_w = 3.3 \times 10^6$ g/mol) as a function of the inert salt concentration: second osmotic virial coefficient (a); radius of gyration and hydrodynamic radius (b); structure sensitive ratio ρ (c).

As shown in Tables 3 and 4, our ρ results for NaPA lie much closer to the theoretically predicted values than the ρ values observed for the neutral polymers do. This small difference between NaPA and neutral polymers may at least in part be attributed to the higher polydispersity of our NaPA samples compared to the narrow distributions of neutral standard polymers [45]. Nevertheless, the drop of ρ observed for NaPA is in agreement with the solvent induced decrease mentioned above [39–42]. This indicates that the NaPA chains undergo a transformation from a self avoiding walk in 0.1 M NaCl (good solvent conditions) to a random walk in 1.5 M NaCl (Θ-conditions), in agreement with the disappearance of the second osmotic virial coefficient.

Having thus identified 0.1 M NaCl and 1.5 M NaCl as a good solvent and a Θ-solvent respectively, the very conditions were selected for measurement of the molar mass dependencies of the light scattering parameters.

Although the second virial coefficient suffered from the largest experimental uncertainty, the same trends occurred as with neutral polymer chains in organic solvents. Under good solvent conditions, a power law of $A_2 \sim M_w^{-0.3}$ could be extracted, which compares to the theoretical limit of $A_2 \sim M_w^{-0.2}$. In 1.5 M NaCl, which is close to a Θ-solvent, a much steeper drop with molar mass was recovered. Noteworthy, NaPA under both solvent conditions [46,47] exhibited A_2 values larger by an order of magnitude if compared to polystyrene as a typical representative for neutral polymers. It is this large increase in A_2 which causes the polyelectrolyte system to approach the limit of $A_2 \sim 0$ at much higher molar mass values than neutral chains do in organic Θ-solvents.

For the size of the polyelectrolyte coils, the following power laws were found:

$$\text{In 0.1 M NaCl}: \quad R_g = 0.0214 \cdot M_w^{0.60} \qquad (13a)$$

$$R_h = 0.0112 \cdot M_w^{0.60}$$

$$\text{In 1.5 M NaCl}: \quad R_g = 0.0374 \cdot M_w\ 0.52 \qquad (13b)$$

$$R_h = 0.0232 \cdot M_w^{0.52}$$

A graphical representation is given in Fig. 4a,b. Clearly, the exponents offer further support for the assumed solvent conditions in 0.1 M NaCl and 1.5 M NaCl.

Accordingly the ρ-ratio was found to be molecular weight independent at each of the two salt levels. The averaged value in 0.1 M NaCl and 1.5 M NaCl is $\rho = 1.84$ and $\rho = 1.53$ respectively. Detailed results are summarized in Tables 3 and 4. The difference of the two values agrees with the salt dependence observed in Fig. 3c.

Table 3
Dilute solution properties of NaPA in aqueous 1.5 M NaCl

Supplier	M_w (g/mol)	R_g (nm)	R_h (nm)	ρ	A_2 (10^{-4} mol cm^3 g^{-2}	k_D (cm^3/g)
PSS	171000	19.2	12.7	1.51	1.24	0.0
Polysciences	473000	27.0	18.5	1.46	0.777	−42.2
PSS	700000	44.0	27.2	1.62	0.0299	−172
Polysciences/PA1	907000	49.3	30.6	1.61	0.923	−120
PSS	2610000	78.4	51.7	1.52	0.564	−249
Polysciences/PA2	3150000	80.6	54.9	1.47	0.0527	−122

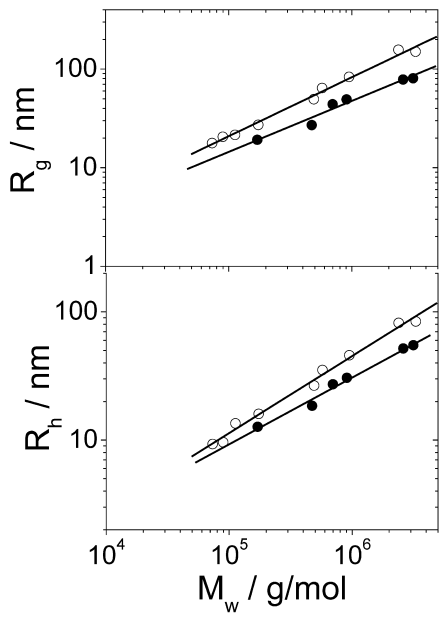

Fig. 4. Radii of gyration R_g and hydrodynamic radii R_h versus weight averaged molar mass of the NaPA chains. The symbols denote experiments in 1.5 M NaCl (●) and 0.1 M NaCl (○), respectively.

3.2. Unperturbed dimensions of NaPA

The unperturbed dimensions of a polymer chain can be expressed either by means of the Kuhn statistical segment of length l_k or in terms of the so called characteristic ratio, corresponding to the coil size divided by the square root of the molar mass. Several literature values are available on l_k and can be compared to our results. One method to evaluate l_k uses Kratky-plots of small angle scattering curves [48,49]. Those plots reveal an upturn at a characteristic value of the scattering vector q^*. The characteristic value q^* can be transformed into l_k according to $l_k = k/q^*$. Depending on the choice of the proportionality constant k, the Kuhn segment length l_k for PA chains varied between $1.6\ \text{nm} < l_k < 2.8\ \text{nm}$. Another route to values of the Kuhn segment length l_k is the application of the hydrodynamic theory of semi-flexible chains according to Yamakaw–Fujii [50] on intrinsic viscosity data. This has been performed by Kitano et al. [9] who measured an extensive set of molecular weights at various levels of an inert salt. Due to the fact that no excluded volume effect was considered in the Yamakawa–Fujii theory, the l_k values fitted by Kitano et al. [9] were apparent in nature except for the highest salt level of 1.5 M NaBr which corresponded to the Θ-state. Here l_k approached 4.0 nm.

Turning to our own data, we can take advantage of having identified 1.5 M NaCl as a Θ-solvent within experimental error, and use the data measured therein for an evaluation of the Kuhn segment length l_k of NaPA. This can be achieved by comparing the corresponding experimental radii of gyration with the predictions of the wormlike chain model according to Eq. (14).

$$R_g^2 = \frac{(z+2)l_k L_w}{(z+1)6} - \frac{l_k^2}{4} + \frac{l_k^3}{4L_w} - \frac{l_k^4(z+1)^2}{8L_w^2 z(z+1)} \times\left[1 - \left(\frac{(z+1)l_k}{(z+1)l_k + 2L_w}\right)^z\right] \quad (14)$$

Eq. (14) represents the z-averaged mean squared radius of gyration for polydisperse wormlike chains [51] with a Schultz–Zimm distribution [52] of the molar mass. In

Table 4
Dilute solution properties of NaPA in aqueous 0.1 M NaCl

Supplier	M_w (g/mol)	R_g (nm)	R_h (nm)	ρ	A_2 (10^{-4} mol cm^3/g^2)	k_D (cm^3/g)
PSS	73000	17.8	9.3	1.91	24.1	88.9
PSS	90000	20.6	9.6	2.15	23.5	169
PSS	113000	21.5	13.5	1.59	15.6	190
PSS	174000	27.2	16.0	1.70	19.1	201
Polysciences	491000	49.4	26.6	1.86	14.3	304
PSS	575000	64.3	35.1	1.83	8.70	203
Polysciences/PA1	950000	83.2	45.8	1.82	11.2	480
PSS	2390000	156.7	82.0	1.91	6.39	998
Polysciences/PA2	3300000	150	84.1	1.78	6.56	1073

Eq. (14), the parameter $z = M_n/(M_n - M_w)$ accounts for polydispersity with M_n the number averaged molar mass of the respective NaPA chains and $L_w = bM_w/M_o$ the weight averaged contour length with M_o the molar mass of a sodium acrylate monomer and $b = 0.259$ *nm* its length [53].

As shown by Fig. 5, the l_k values extracted in 1.5 M NaCl are independent of the molar mass of NaPA samples in accord with the findings of aqueous 1.5 M NaCl to be close to a Θ-solvent. Thus an averaged value of $l_k = 4.2$ *nm* can be calculated. This value is in close agreement to the one evaluated by Kitano et al. [9] from intrinsic viscosity data but is somewhat larger than the result from small angle scattering curves [48,49]. At this point, it is worth referring to the data on NaPA measured by Wiegand et al. [25] in aqueous 1 M NaCl. Values for l_k could be extracted from their data in the same way as described above. Although the salt level applied is already lower than 1.5 M, still no molecular weight dependence becomes noticeable. More important, averaging of the respective values leads to $l_k =$ 3.4 *nm* in reasonable agreement to our value. Obviously, the solvent quality only gradually increases if the NaCl content is lowered.

It is interesting now to estimate l_k values also from our results in 0.1 M NaCl, which is a good solvent. A similar procedure was suggested first by Reed et al. [54], who pointed out that the Kuhn segment length l_k increases with molecular weight due to the incorporation of excluded volume effects rendering l_k apparent in nature (l'_k). The results are also included in Fig. 5. In analogy to the $M_w^{1/2}$ dependence of $[\eta]/M_w^{1/2}$ discussed by Burchard [55] and Stockmayer and Fixman [56], l'_k is plotted versus $M_w^{1/2}$. As expected, for good solvent conditions, l'_k increases with $M_w^{1/2}$. However, extrapolation of the l'_k values to $M_w^{1/2} = 0$ in Fig. 5 leads to a limiting value, free of excluded volume effects which within experimental uncertainty agrees with the averaged value, determined in 1.5 M NaCl.

Further support for this behaviour can be received from the hydrodynamic radii, measured under both solvent conditions. Inspired by the work of Stockmayer and Fixman [56], Cowie and Bywater [57] suggested a plot of $R_h/M_w^{1/2}$ versus $M_w^{1/2}$ according to

$$R_h/M_w^{1/2} = K_1 + K_2\, M_w^{1/2} \tag{15}$$

Corresponding results for our NaPA measurements are summarised in Fig. 6. As expected, a molecular weight independent value of $R_h/M_w^{1/2} = 0.031$ [nm/(g/mol)$^{0.5}$] was found in 1.5 M NaCl. Contrary to the situation in 1.5 M NaCl, the data extracted in 0.1 M NaCl showed a significant dependence on the molar mass. As already noticed for l_k, extrapolation of $R_h/M_w^{1/2}$ to $M_w^{1/2} = 0$ yield a value which is compatible with the $R_h/M_w^{1/2}$ value averaged in 1.5 M NaCl. Although data in Figs. 5 and 6 suffer from a comparatively large scatter, both figures indicate that at least in the range of 0.1 M $\leq C_s \leq$ 1.5 M experimental data can be interpreted by the same unperturbed dimensions.

3.3. Excluded volume effects as a function of the inert salt level

For neutral polymers, excluded volume effects can be described by the so called expansion coefficient α, which is expressed in terms of R_g or R_h

$$\alpha_g = R_g/R_g(\Theta) \tag{16a}$$

$$\alpha_h = R_h/R_h(\Theta) \tag{16b}$$

In Eq. 16(a) and (b), the denominator represents the geometric or hydrodynamically effective coil dimensions under good solvent conditions respectively. In both ratios, they are compared to the unperturbed dimensions measured in a Θ-solvent. Based on two parameter theory [58], this ratio can be related to the molar mass according to

$$\alpha_g^5 - \alpha_g^3 = \omega_o N^{0.5} \tag{17}$$

where N is the number of Kuhn segments with step length l_k. The constant ω_o depends on the Flory–Huggins interaction parameter χ according to

$$\omega_o = \frac{134}{105}\left(\frac{3}{2\pi}\right)^{3/2}\left(\frac{1}{2} - \chi\right) \tag{18}$$

Electrostatic interactions amplify the excluded volume

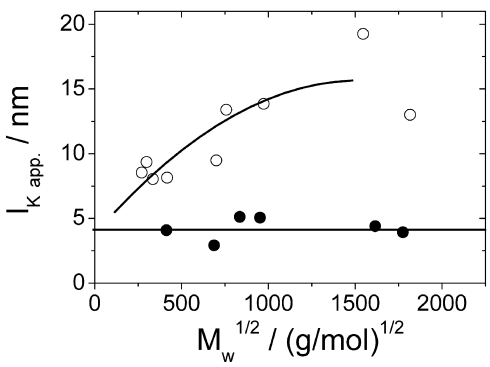

Fig. 5. Kuhn segment length in 1.5 M NaCl (●) and of the apparent Kuhn segment length in 0.1 M NaCl (○) determined according to Eq. (14) as a function of the square root of the weight averaged molar mass. The lines serve as a guide for the eye.

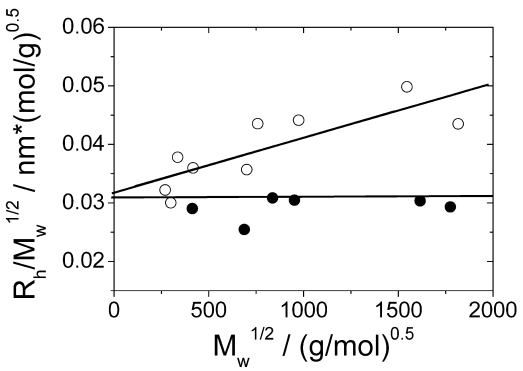

Fig. 6. Cowie–Bywater plot with R_h in 1.5 M NaCl (●) and 0.1 M NaCl (○). The lines are linear fits.

effect on chain dimensions and/or the intrinsic chain stiffness. Various procedures have been suggested in order to account for these additional interactions.

Muthukumar et al. [23,59,60] applied a variational procedure to a polyelectrolyte chain which consists of monomers with length b and valence Z, assuming uniform chain expansion. The effective charge of the monomer is expressed as fZ with f the effective degree of ionization. The polyelectrolyte chain is modeled as a sequence of N Kuhn segments of length l_k. The electrostatic interactions were accounted for by three different factors: (i) The effective linear charge density of the chain fZ/b; (ii) the solvent mediated range of electrostatic interactions via the Bjerrum length l_B; (iii) electrostatic screening due to addition of inert salts composed of m different ion species via the inverse Debye length κ

$$\kappa^2 = 4\pi l_B \sum_i^m Z_i^2 C_i. \tag{19}$$

In the limit of $\kappa^2 b^2 N\alpha^2/6 \gg 1$, their calculations resulted in an extension of Eq. (17) [23,61]

$$\alpha_g^5 - \alpha_g^3 = \left[\omega_o + \frac{134}{35}\sqrt{\frac{6}{\pi}}\cdot\frac{l_B Z^2 f^2}{l_k \kappa^2 b^2}\right]\sqrt{N} \tag{20}$$

Prior to application of Eq. (20) values have to be assigned to the following parameters: κ is calculated by Eq. (19) with C_i equal to 1.5 M or 0.1 M of NaCl; 0.72 and 0.259 nm are used for the Bjerrum length l_B and the monomer length b respectively; the Kuhn length $l_k = 4.2\,nm$ was evaluated from the experimental R_g^2 data in 1.5 M NaCl by means of Eq. (14).

A proper application of Eq. (20) to our data rests on the following assumptions: the R_g^2 values of the NaPA chains in 1.5 M NaCl correspond to the unperturbed dimensions and provide an appropriate denominator for α_g. The Kuhn segment length l_k determined from the very data remains unaffected by a change of the effective degree of ionization fZ of the chain. In other words, the intrinsic chain stiffness is independent of the NaCl concentration C_s. The latter assumption may become increasingly questionable, as C_s decreases and the impact of electrostatic interaction icreases [62,63]. However, the above presented results on unperturbed dimensions clearly support both assumptions, if $C_s \geq 0.1$ M.

We can now proceed to apply Eq. (20). Two procedures are possible. One procedure is to plot the molar mass dependent coil expansion received in 0.1 M NaCl as $\alpha_g^5 - \alpha_g^3$ versus $N^{0.5}$. At 1.5 M NaCl, this slope is zero by definition. Under the assumption of a unique ω_o term, f is the only other parameter left to be adjusted in order to reproduce the slopes in 0.1 M NaCl. The second procedure uses the salt dependent data, measured with sample PA2. Now, an expansion coefficient α_g can be calculated as a function of κ^2 where κ^2 is related to C_s according to Eq. (19). Again, a fit of Eq. (20) to the data yield a value for f and ω_o.

Estimation of fit parameters from molar mass dependent data resulted in $f = 0.2$ and $\omega_o = -0.03$. Unfortunately, corresponding data for $\alpha_g^5 - \alpha_g^3$ suffered from a large experimental uncertainty and we did not consider any further this procedure. A more precise estimate for f and ω_o was expected from an independent series of experiments on the solution behaviour of sample PA2 ($M_w = 3.3 \times 10^6 \times$ g/mol) at a variable inert salt content. The respective data, which covered a salt regime of 0.01 M$\leq C_s \leq$1 M NaCl, are summarized in Table 5. It is worth being emphasized that the values for the molar mass agreed within 10%, confirming the liability of Eq. (3). The respective second virial coefficient started with a value of $A_2 \sim 30 \times 10^{-4}$ cm^3 mol/g^2 at $C_s = 0.01$ M NaCl and decreased by more than an order of magnitude while the salt level was increased to 1 M. Close to $C_s = 1.5$ M NaCl, A_2 gradually approached 0. Further discussion will be focused on the behaviour of the mean square radius of gyration R_g.

If R_g data in the range of 0.1 M$\leq C_s \leq$1.0 M were used for a fit according to Eq. (20), $f = 0.184$ and $\omega_o = -0.044$ were received as fit parameters. As is shown in Figs. 7 and 8, the resulting theoretical curves led to a satisfactory description of data only, for $C_s \geq 0.1$ M NaCl. A perfect description of experiments at $C_s < 0.1$ was achieved with $f = 0.256$ and $\omega_o = -0.614$ resulting from a fit which was restricted to the low salt regime of 0.01 M$\leq C_s \leq$0.1 M NaCl accordingly. This time, the corresponding theoretical curve exceeds experimental data at the high salt regime. A third fit to all data which forces ω_o to a value of -0.044 again recovered experimental data at the low salt regime and approached the proper unperturbed limit but did not significantly improve the overall description otherwise.

Focusing on the inert salt regime of $C_s > 0.1$ M NaCl in the first place, the following aspects become obvious: (i) the effective degree of ionization is smaller than the value of $f = b/l_B = 0.259$ nm/0.712 nm $= 0.36$ corresponding to the Manning counterion condensation limit for monovalent counterions [62]. This has been observed already by Schmidt et al. [23] for polycations. (ii) Description of the

Table 5
Dilute solution properties of sample PA2 as a function of the NaCl concentration denoted as C_s

C_s (M)	M_w (10^6 g/mol)	A_2 (10^{-4} mol/cm^3 g^2)	R_g (nm)	R_h (nm)	ρ	k_D (cm^3/g)
0.01	3.33	30	275	129	2.13	5000
0.03	3.29	15	202	117	1.73	4500
0.06	3.62	10	188	106	1.78	2500
0.1	3.25	7.3	158	87	1.82	1152
0.25	3.31	4.0	130	70	1.86	434
0.5	3.37	1.45	104	64	1.63	235
0.75	3.23	1.62	96	58	1.66	120
1.0	3.36	1.20	86	53	1.62	−74

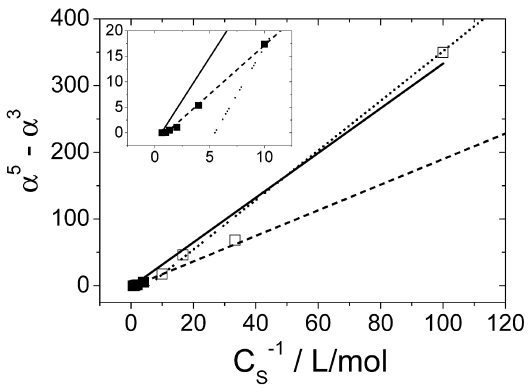

Fig. 7. Flory-plot of the coil expansion $\alpha_g^5 - \alpha_g^3$ versus C_s^{-1} for sample PA2. The lines represent fits according to Eq. (20): (· · ·) fit to the open squares corresponding to $C_s \leq 0.1$ *M* NaCl with $f = 0.256$ and $\omega_o = -0.614$; (· · ·) fit to the filled squares corresponding to 1.0 M $> C_s \geq 0.1$ M NaCl with $f = 0.184$ and $\omega_o = -0.044$; (—) fit to all data points with the excluded volume parameter forced to $\omega_o = -0.044$ resulting in $f = 0.243$. The inlay is a detail of the high salt regime.

coil expansion of polyelectrolytes does not require introduction of an electrostatic contribution to the persistence length as long as $C_s \geq 0.1$ M. For the present system, a unique value of $l_k = 4.2$ nm and a variable excluded volume parameter is sufficient to describe dilute solution behaviour of NaPA in saline solutions if the content of added salt does not fall below 0.1 M. The excluded volume parameter comprises a constant, intrinsic part of $-0.04 > \omega_o > -0.05$ corresponding to the neutral monomer and an additional, variable electrostatic contribution which accounts for the salt dependent screening of electrostatic interaction via κ^2. (iii) The negative value of ω_o indicates the existence of Θ-conditions at a finite concentration of added salt. If the regime of inert salt is decreased below 0.1 M NaCl, Eq. (20) starts to deviate from experiment. Agreement in the low salt regime is recovered with a slightly increased effective degree of ionisation f. However this improvement can only be achieved at the expense of the validity of ω_o which deteriorates towards $\omega_o = -0.6$.

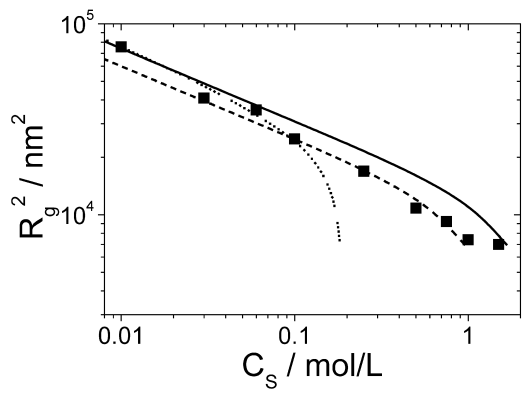

Fig. 8. Mean square radius of gyration R_g^2 versus C_s for sample PA2. The theoretical curves are calculated from the fits which are represented in Fig. 7.

4. Conclusions

The molecular weight dependence of the radius of gyration R_g and the hydrodynamic radius R_h obeys a power law with an exponent of $\nu = 0.6$ in 1.5 M NaCl and $\nu = 0.52$ in 0.1 M NaCl. The exponents confirm the picture of 1.5 M NaCl being close to a Θ-solvent and 0.1 M NaCl being a good solvent for NaPA. The dilute solution behaviour of NaPA in saline solutions can be described by a set of two parameters if $C_s \geq 0.1$ M NaCl, a Kuhn segment length with a single value of $l_k = 4.2$ nm independent of the amount of salt and a modified excluded volume parameter with a single value for ω_o plus an extra term which accounts for the variations due to addition of an inert salt [23,59,60]. Applicability of this approach [23,59,60] to NaPA in saline solutions is restricted to an inert salt regime of one order of magnitude relative to C_s which generates the Θ-conditions. Although being at the upper limit, the present value for $l_k = 4.2$ nm is compatible with literature data which spread over a range of 1.6 nm $< l_k <$ 4 nm. Description of the NaPA dimensions with a constant Kuhn segment length for $C_s \geq 0.1$ M NaCl is supported by the results of Muroga et al. [48] based on SAXS curves. Their values are 25–50% smaller than the present value, but extend on a salt range of 0.01 M$\leq C_s \leq 0.1$ M where an l_k value was found to be constant and equal to the one for neutral polyacrylic acid. This is expected under the assumption of a counterion condensation limit which provides an effective charge density independent of the concentration of an added salt.

Acknowledgements

Financial support by the Deutsche Forschungsgemeinschaft within the Schwerpunktprogramm ‘Polyelektrolyte mit definierter Molekülarchitektur’ SPP 1009 is greatly acknowledged. The authors are indebted to S. Wiegand for helpful comments and Professor M. Schmidt for many discussions and access to their Scan Ref instrument.

References

[1] Flory PJ, Osterheld JE. J Phys Chem 1954;58:653.
[2] Orofino TA, Flory P. J Phys Chem 1959;63:283.
[3] Takahashi A, Yamori S, Kagawa I. Kogyo Kagaku Zasshi 1962;83:11.
[4] Takahashi A, Nagasawa M. J Am Chem Soc 1964;86:543.
[5] Noda I, Tsuge T, Nagasawa M. J Phys Chem 1970;74:710.
[6] Kay P, Treloar FE. Makromol Chem 1974;175:3207.
[7] Hara M, Kakajima A. Polym J 1980;12:701.
[8] Nagasawa M, Noda I, Kitano T. Biophys Chem 1980;11:435.
[9] Kitano T, Taguchi A, Noda I, Nagasawa M. Macromolecules 1980;13:57.
[10] Nagasawa M. In: Nagasawa M, editor. Studies in polymer science, vol. 2. Amsterdam: Elsevier; 1988. p. 49. and references therein.
[11] Debye P. J Phys Colloid Chem 1947;51:18.

[12] Peterlin A. J Chem Phys 1955;23:2464.
[13] Kratky O, Porod G. Rec Trav Chem 1949;68:1106.
[14] Förster S, Schmidt M. Advan Polym Sci 1995;120:51.
[15] Raziel A, Eisenberg H. Isr J Chem 1971;11:183.
[16] Wang L, Yu H. Macromolecules 1988;21:3498.
[17] Tanahatoe JJ, Kuil ME. J Phys Chem A 1997;101:8389.
[18] Griebel Th, Kulicke W-M, Hashemzadeh A. Colloid Polym Sci 1991; 269:113.
[19] Dautzenberg H, Görnitz E, Jäger W. Macromol Chem Phys 1998;199: 1561.
[20] Chisaka S, Norisuye T. J Polym Sci, Part B: Polym Phys 2001;39: 2071.
[21] Fisher LW, Sochor AR, Tan JS. Macromolecules 1977;10:949.
[22] Beer M. PhD Thesis, University of Bayreuth; 1996.
[23] Beer M, Schmidt M, Muthukumar M. Macromolecules 1997;30:8375.
[24] Yashiro J, Norisuye T. J Polym Sci B: Polym Phys 2002;40:2728.
[25] Reith D, Müller B, Müller-Plathe F, Wiegand S. J Chem Phys 2002; 116:9100.
[26] Brüssau R, Goetz N, Mächtle W, Stölting J. Tenside Surf Det 1991;28: 396.
[27] Kato T, Tokuya T, Nozaki T, Takahashi A. Polymer 1984;25:218.
[28] Zimm BH. J Chem Phys 1948;16:1093.
[29] Berry GC. J Chem Phys 1966;44:4550.
[30] Provencher SW. Comput Phys 1982;27:213.
[31] Provencher SW. Comput Phys 1982;27:229.
[32] Koppel DE. J Chem Phys 1972;57:4814.
[33] Burchard W, Schmidt M, Stockmayer WH. Macromolecules 1980;13: 580. Burchard W, Schmidt M, Stockmayer WH. Macromolecules 1980;13:1265.
[34] King TA, Knox A, Lee WI, McAdam JDG. Polymer 1973;14:151.
[35] Frost RA, Caroline D. Macromolecules 1977;10:616.
[36] Han C. Polymer 1979;20:259.
[37] Mandema W, Zeldenhurst H. Polymer 1977;18:835.
[38] Appelt B. PhD Thesis, University of Mainz; 1977.
[39] Akcasu AZ, Benmouna M. Macromolecules 1978;11:1193.
[40] Barrett AJ. Macromolecules 1984;17:1561.
[41] Huber K, Burchard W, Akcasu AZ. Macromolecules 1985;18:2743.
[42] Burchard W. Advan Polym Sci 1983;48:1.
[43] Vrentas JS, Liu HT, Duda JC. J Polym Sci: Polym Phys Ed 1980;18: 633.
[44] Schmidt M, Burchard W. Macromolecules 1981;14:210.
[45] Burchard W, Schmidt M, Stockmayer WH. Macromolecules 1980;13: 1265.
[46] Huber K, Stockmayer WH. Macromolecules 1987;20:1400.
[47] Einaga Y, Fumiaki A, Yamakawa H. Macromolecules 1993;26:6243.
[48] Muroga Y, Noda I, Nagasawa M. Macromolecules 1985;18:1576.
[49] Plestil J, Ostanevich YuM, Bezzabotonov VYu, Hlavatá D, Labsky J. Polymer 1986;27:1241.
[50] Yamakawa H, Fujii M. Macromolecules 1973;6:407.
[51] Oberthür RC. Makromol Chem 1978;179:2693.
[52] Zimm B. J Chem Phys 1948;16:1099.
[53] van Rijn CJ, Jesse W, de Bleijser J, Leyte JC. J Phys Chem 1978;91: 203.
[54] Reed WF, Ghosh S, Medjahdi G, Francois J. Macromolecules 1991; 24:6189.
[55] Burchard W. Makromol Chem 1961;50:20.
[56] Stockmayer WH, Fixman M. J Polym Sci, Part C 1963;1:137.
[57] Cowie JMG, Bywater S. Polymer 1966;6:197.
[58] Flory P. Principles of polymer chemistry. Ithaca: Cornell University Press; 1953. [Chapter 14].
[59] Muthukumar M. J Chem Phys 1987;86:7230.
[60] Muthukumar M. J Chem Phys 1996;105:5183.
[61] Flory PJ. J Chem Phys 1953;21:162.
[62] Odijk T, Houwaart AC. J Polym Sci: Phys Ed 1978;16:627.
[63] Skolnick J, Fixman M. Macromolecules 1977;10:944. Skolnick J, Fixman M. Macromolecules 1978;11:863.